

Impact of Quantum Conductivity on a Reconfigurable Single Wall Carbon Nanotube Dipole Performance at Optical Frequency Bands

Muhanad M. Jameel* and Jawad A. Hasan

Electronic and Communication Department, Institute of Laser for Postgraduate Studies, University of Baghdad, Iraq

ABSTRACT: The proposed antenna system integrates advanced materials electromagnetic properties tuning to allow real-time steering to the antenna main beam direction. We explore a tuning mechanism based on changing the chemical potential differences (μ_c), through including a chiral single wall carbon nanotube (SWCNT) structure with a plasmonic resonance effect at the optical regime. Such change in the value of μ_c realizes a manipulation in the angular emission pattern change to enhance the beamforming capabilities to the desired requirements. This steerability provides substantial benefits for applications such as optical communication systems. The obtained results validate that the proposed nano-dipole antenna shows significant improvements over other traditional antennas in terms of size reduction with acceptable radiation efficiency, directivity, and tunability. The integration of the proposed design within next optoelectronic generations can floor the way to the compact, high-performance systems with enhanced capabilities for optical communication systems and photonic circuitry. This study presents a steerable plasmonic nano-dipole antenna with dynamic electromagnetic radiation control, designed for modern communication. The antenna operates across a wide frequency range, with a primary focus on the visible spectra 300 THz to 700 THz. By utilizing resonant plasmonic effects, the antenna achieves a radiation efficiency of 57% and a directivity of 4.5 dBi. We introduce a beam-steering mechanism that enables angular radiation steering up to $\pm 25^\circ$ from the central axis. Control mechanisms include electrical tuning via applied μ_c voltage from 0 V up to 1 V and optical tuning using laser excitation around 600 THz. Simulations confirm that beamwidth narrows from 30° to 10° at resonance, enhancing spatial precision. The validated results show a tunability of 200 THz in the operational wavelength, with a response S_{11} below -10 dB. These features demonstrate that the antenna operation has a potential for integration into next-generation optoelectronic devices, offering compact and efficient solutions for wireless communication, remote sensing, and optical imaging systems. This is achieved by leveraging the resonant interaction between surface plasmon polaritons and nano-dipole geometry, and we demonstrate the ability to achieve highly directional and tunable radiation across a wide range of frequencies, including visible and near-infrared spectra.

1. INTRODUCTION

Plasmonic nano-dipole antennas have emerged as powerful tools for manipulating electromagnetic waves at the nanoscale, enabling novel functionalities in modern technological applications. Many researchers have utilized nanomaterials in their studies for realizing modern optical antennas. For example, the design proposed in [1] was developed to structure a dipole antenna based on single wall carbon nanotube (SWCNT) of two different indices (10,10) and (21,21). In [2], graphene-based antennas were suggested to employ transceivers in special frequency-beam reconfigurability in the terahertz range. Another design of optical antenna was formed by creating a rectifying diode at the interface between an atomic force microscope (AFM) metal probe and an SWCNT, using a conductive AFM nano-probe in contact with two device structures, one with an SWCNT on a CuO/Cu substrate and the other with an SWCNT on a SiO₂/Si substrate. The electrical and optical characteristics have been examined [3]. The multiwall carbon nanotubes (MWCNTs) used to engineering rectangular patch

antenna which assist in Covid-19 identification checkup, and because they were very conductive, every nanotube reflects electromagnetic waves differently, which affected the bandwidth expansion. The proposed antenna operated at 6.63 GHz, 7.291 GHz, 7.29 GHz, and 7.22 GHz [4]. The composite material structure composed of carbon nanotubes (CNTs) encased in polyaniline (CPC) for innovative CPC materials, the mathematical model for measuring complex conductivity, relative permittivity, and plasma frequency was investigated and developed [5]. A higher light coupling efficiency was the target in building the antenna which accomplished ultra-efficient impedance matching between the antenna and SWCNTs by integrating a bottom metal plane at a specific distance from the SWCNT film and optimizing the antenna geometries. As a result, the absorptance of the junction region was further enhanced by 21.3 times and reached 13.5%, which is more than three orders of magnitude higher than that of the device without the engineered antenna [5]. Single-walled carbon nanotubes (SWCNTs) work well for self-powered thermal detectors at room temperature in the far-infrared (THz) range because they are very stable and do not hold a lot of heat. It was

* Corresponding author: Muhanad Musa Jameel (eng.muhanad88@gmail.com).

suggested that a bowtie antenna stereo structure with a horizontally aligned SWCNTs film could be used to improve the polarization extinction ratio (PER) and the sensitivity of carbon nanotube far-infrared detectors. This allowed us to create new resonance modes and gain mechanisms [7]. It was constructed carbon nanotube-coupled nano-antennas that will radiate light lamp (LL) plasmons into the distant field, and as a result, the far- and mid-infrared spectra can be selectively illuminated at wavelengths using LL-based infrared light-emitting diodes (IRLEDs) [8]. Regarding optical and thermal performance, a CNT film with optimal shape was used for a polyethylene terephthalate (PET) sensor structure with appropriate dimensions $50\ \mu\text{m}$ – $70\ \mu\text{m}$ to operate from 300 THz to 600 THz for a multi-function of detection process, including acoustic and electromagnetic signals. This improved the detection sensitivity by around 13 times compared to a single-element PET sensor [9]. The improved efficiency metrics for coated and uncoated carbon nanotube dipole antennas were discovered at various length ranges and constant radii efficiency found about 59%, providing a useful model for solar cells, biomedical engineering, sensors, and wireless communication technologies [10]. Antenna applications based on materials include SWCNT composites covered with a thin layer of substance (copper, silver, or graphite) to create new nanomaterials with enhanced electromagnetic characteristics [11]. The radiation properties of SWCNTs were found as very substantial features to enhance the performance of dipole nano-antennas for various applications [12]. Another design proposed in [13] based on a nano-antenna was designed with dimensions $130 \times 130\ \text{nm}^2$ on a substrate of glass which had a thickness 112 nm with an area of $40 \times 2.5\ \text{nm}^2$ to achieve a radiation efficiency around 96.54% with a resonance around 182 THz to offer a bandwidth from 160 THz to 207 THz. Two connected V-shaped arms of cross dipole nano-antenna produced a directivity of 8.79 dBi which was initiated from a unidirectional radiation pattern at 1550 nm [14]. A broadband optical nano-antenna was developed in [15] to cover the spectral width from 666 nm to 6000 nm to be employed in nano-photonics applications with a reasonable gain up to 11.4 dBi. For optical communication in free space, a nano-antenna based on a metamaterial structure was proposed in [16] to control the electromagnetic beam directivity sub-wavelength variation within the plasmonic resonance [16]. Another design was proposed in [17] based on nano hybrid plasmonic effects with an area of $1100 \times 800\ \text{nm}^2$ to feed a hybrid plasmonic waveguide at the frequency range from 160 THz to 240 THz to realize a maximum gain of 7 dBi and an efficiency of 94%. Several designs of hybrid plasmonic nano-antenna were considered in [17]; the designs were constructed from different patch structures mounted on a silicon substrate including hexagonal, circular, rectangular, and elliptical geometries to enhance radiation at the desired specifications [18]. Another antenna design was structured as a crown-shaped Acer leaf with a Y-shaped transmission line based on a quantum capacitor mounted on a silicon substrate with a partial ground plane; the resulting antenna structure was $49 \times 49\ \text{nm}^2$ with thickness of 1 nm [19]. A flower-shaped silver nano-dipole antenna was examined on a silicon dioxide substrate for optical wireless communication as discussed in [20] to cover the fre-

quency ranges from 170 THz to 271 THz for optical communication systems.

The article in [21] discusses the creation of photoluminescent erbium-doped silicon nano-antennas, a step towards silicon-based optoelectronic systems. The process involves electron beam lithography and laser annealing, optimizing the silicon nanoparticle geometry to enhance photoluminescence intensity by up to 40%. Nano-photonics can improve chiral molecules' weak signal in circular dichroism spectroscopy experiments by increasing optical chirality in near-field antennas. However, measuring near-field optical chirality is complex. A single measurement of far-field circular polarization quantifies near-field circular dichroism (CD) enhancements, predicting optimal antenna response for enhanced chiral sensing. This approach can be useful for the characterization of devices enhancing CD from a single far-field Stokes measurement [22]. Laser fields reveal matter's attosecond and femtosecond responses in photoelectrons and high-harmonic photons which was discussed in [23]. Electron emission and high-order harmonics probe laser-matter interaction in gas molecules and bulk solids. In nanoscale solids, electron emission reveals localized and inhomogeneous near fields, affecting high-order harmonics. This extends electron-photon perspective to nanoscale systems.

This study presents the design and characterization of a steerable plasmonic nano-dipole antenna capable of dynamically controlling the radiation pattern directionality. For this, the paper is oriented to realize the use of an SWCNT structure to control the electromagnetic properties of a dipole antenna based on copper nano-wire around 600 THz. The paper is divided into the following sections. In Section 2, an SWCNT structure is discussed with plasmonic features. The antenna geometry and material properties are explored in Section 3. The antenna design methodology is discussed in Section 4. The effects of changing the μ_c are explored in Section 5. The paper is concluded in Section 6.

2. SWCNT STRUCTURE AND THE PLASMONIC EFFECTS

SWCNT structures are an exceptional shape of carbon nanotubes, which are formed from a single graphene layer rolled on a cylindrical shape with diameters of 1 nm to realize lengths in the range a high aspect ratio from several "nm" to some "cm" [21]. SWCNT structures own remarkable mechanical, electrical, and optical properties to attribute 1D structures of ballistic conductors [21]. Based on rolling the graphene layer exhibits the metallic, semiconducting, isolative behavior, which directly impacts on their electronic properties [22]. In Fig. 1, the structure of SWCNT with different rolling directions to form Zigzag, Armchair, Chiral, realistic, and length details.

The plasmonic effects of SWCNT are one of its best features. These happen when the conduction electrons oscillate at the same frequency as the light that hits them, creating plasmons, which are collective electron oscillations. For SWCNT structures, the plasmonic performance is inclined by the SWCNT diameter and tunable electronic properties. Plasmon resonances in SWCNTs can be excited by incident electromagnetic radiation, leading to enhanced optical absorption and

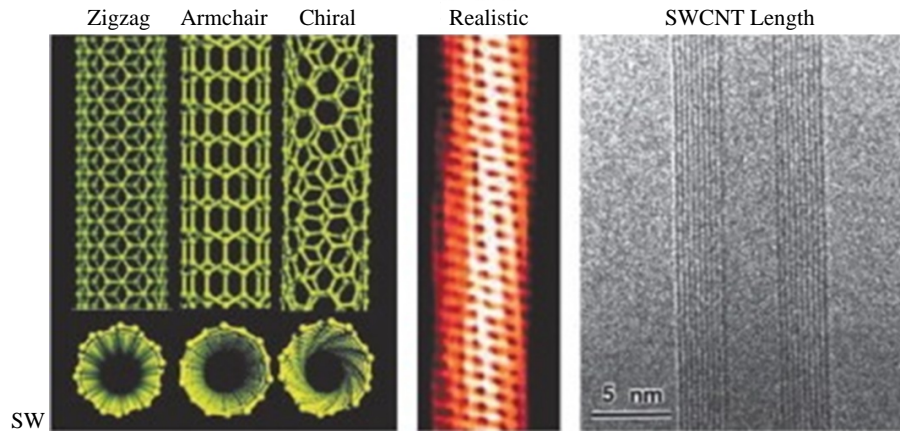


FIGURE 1. SWCNT geometry and details of rolling [21].

scattering. These effects are mainly marked in conductive and semiconductive SWCNT structures, where the free electrons facilitate plasmon generation and support strong electromagnetic fields at the nanotube surface. These plasmonic behaviors can be explored for individual SWCNT within the range of optical regimes as seen in Fig. 2 [23]. Plasmonic properties of SWCNT structures are capable for modern applications including sensors, photodetectors, optoelectronic devices, and nano-antennas due to their enhanced light-matter fields interactions. The (11,8) index of single-walled carbon nanotubes (SWCNTs) outlines its chiral vector, revealing the process of convolving a graphene sheet to form the nanotube. This index defines the chirality, diameter, and electrical characteristics of the nanotube. The designation (11,8) denotes a chiral nanotube having a configuration that is neither exclusively zigzag nor armchair, leading to distinctive optical and electrical properties. From these indices, we can find the diameter and chiral angle, which change how the SWCNT interacts with electromagnetic fields (Fig. 2).

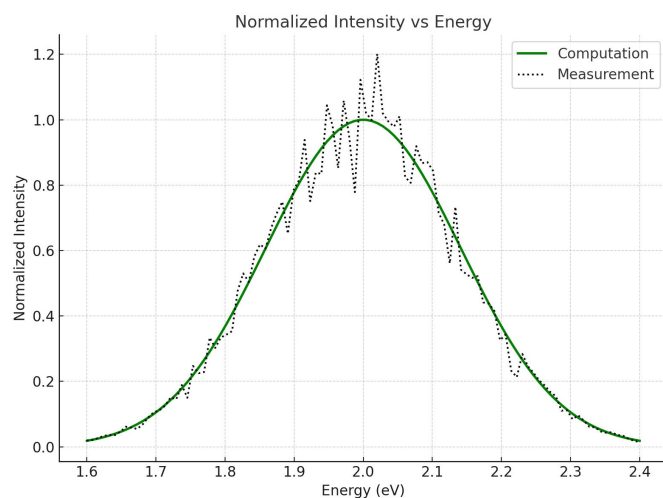


FIGURE 2. Normalized scattered electromagnetic field for individual SWCNT based on (11,8) index [23] based on simulated and measured results.

It is good to mention that the plasmonic resonance frequency of SWCNTs varies depending on their structural and electronic properties, as well as environmental factors [10]. Key determinants of plasmonic frequency include the electronic type of SWCNT, nanotube diameter and chirality, environmental dielectric constant, and the length of the SWCNT. Metallic SWCNTs typically exhibit higher frequencies than semiconducting SWCNTs, arising from intraband transitions in metallic tubes and interband transitions in semiconducting tubes [23]. Nanotube diameter and chirality scale inversely with the nanotube's diameter, with smaller diameters leading to higher frequencies [11]. A higher dielectric constant reduces plasmonic resonance frequency. SWCNTs exhibit higher plasmon frequencies due to quantum confinement effects [3]. Typical plasmonic frequency ranges include the Terahertz (THz) range, where intraband plasmons are typically in the 0.1 to 10 THz range [2], and the infrared to visible range [10], where plasmons resulting from interband transitions occur at frequencies ranging from far-infrared and visible regions [23]. Tuning frequency can be achieved through doping, hybridization, and geometric modifications [1].

Another aspect of the study involves measuring the normalized scattered electromagnetic field for an isolated SWCNT using single-particle spectroscopy. This can be achieved by exciting the isolated SWCNT by optical spectroscopy devices to detect the plasmonic properties. During the sample preparation, the individual SWCNT was isolated from other nanotubes by selective dispersion or chemical functionalization. The SWCNT was mounted on a transparent substrate based on SiO_2 to support the SWCNT during the measurements. In this process, a laser excitation was used with a wavelength near the resonant plasmon frequency of the considered SWCNT. Collecting the scattered light into a spectrometer can be analyzed from the dark-field microscope where such arrangement maximizes the scattered signal relative to the background.

Find the plasmonic peaks in the scattering spectra that match the resonant modes of the SWCNT under consideration. Model the scattering response of the SWCNT under consideration by computational techniques (e.g., numerical simulation by setting the boundary condition). The simulations shed light on the res-

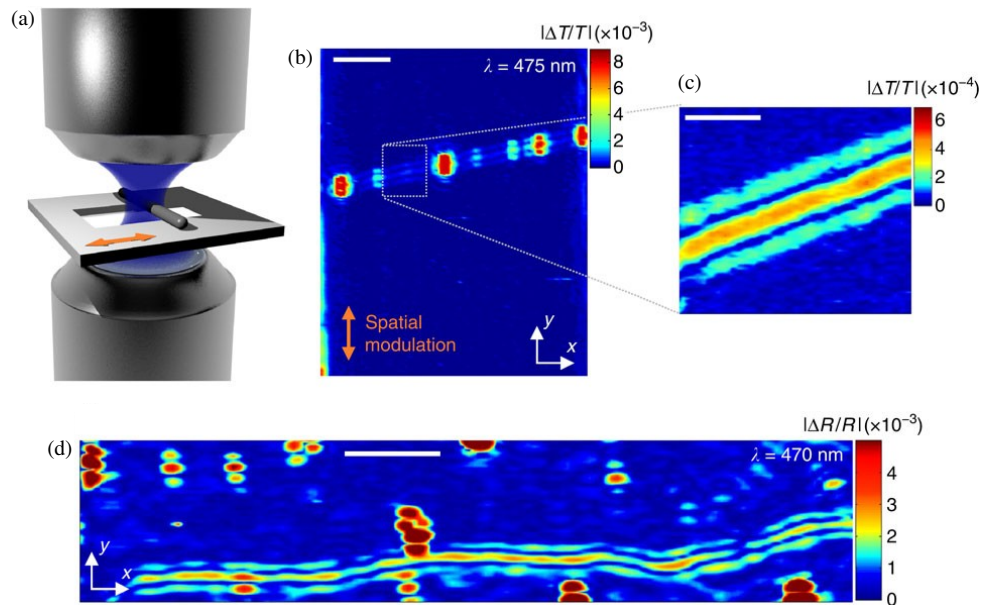


FIGURE 3. The measurement spectroscopy setup of the isolated SWCNT [24].

onant plasmon modes unique to this chirality and aid in the interpretation of the experimental findings. A normalized scattered electromagnetic field spectrum can be obtained by using a laser to excite a single (11, 8) SWCNT (see Fig. 3), collecting the scattered field, and normalizing it against the incident field. By providing a distinct spectrum signature that can be compared to theoretical expectations, the chirality-specific resonant plasmonic modes shed light on the SWCNT's electrical and plasmonic characteristics.

3. ANTENNA GEOMETRICAL DETAILS AND MATERIAL PROPERTIES

The proposed antenna in this study is constructed as a traditional dipole structure of two arms as illustrated in Fig. 4. However, each antenna arm is mainly constructed from three SWCNT sectors filled with gold wire and separated with gold disks as seen in Fig. 4. The antenna is fed by a virtual optical source for pumping the electromagnetic field toward the antenna arms. Therefore, the gold wire is introduced to serve two purposes: facilitating the current flow toward the SWCNT section and keeping the plasmonic current flow within a high conduction and displacement density. This behavior is based on the surface energy, which is comparable to the volumetric density [21]. Next, the use of SWCNT section is adopted to allow the frequency tuning through tunneling the ballistic conductivity by controlling the quantum motion of the electronic passage with a limited aspect ratio. This configuration enables the application of high current densities with minimal deviation from the axial direction, optimizing charge motion along the SWCNT surface [22]. With all this to be achieved with a semi-classical approach based on Maxwell's Equations, two main points must be addressed: First, the quantum model of each material, including the gold sections, must be accurately invoked to model the behavior of the antenna effectively as established in the lit-

erature. Second, apply the realistic geometry of the SWCNT, despite δ - π bonds, to maintain the exact motion of the electron charges in accordance with ballistic theory. Our proposed approach was previously discussed with other research groups that published a similar idea previously [23]. However, some of them did not consider the facts of integrating both the quantum conductivity model and realistic geometry. Such ignorance for this combination leads to ignoring one of the effective parts of the physical phenomena which was explained by the quantum capacitor and kinetic inductor. Nevertheless, neglecting quantum conductivity implies overlooking the effects of dispersion that could lead to diminished confidence in the obtained results. Therefore, this research aims to combine both aspects by invoking the quantum conductivity of the nanomaterial and considering the realistic geometry during the simulation study. During that, the use of SWCNT is found to be very effective in tuning the antenna performance based on the variation in effects of the chemical potential difference.

It is important to mention that the plasmonic resonance is independent of the SWCNT length, because it is an inherent signature that comes from the electron motion on the SWCNT surface. However, the increase of the SWCNT length increases the flexomagnetic field intensity to realize an enhanced antenna directivity and running effects. Also, it is very important to select the antenna resonant frequency within the bandwidth at which the losses are minimum.

It is good to mention that we conducted, in this work, three sections in each arm to ensure an antenna array performance but from another technique [11]. Such geometry would be useful for us to control the antenna beam steering as will be seen later. Nevertheless, each arm is considered according to $\lambda/4$ to ensure the antenna resonance around the desired frequency band of interest without effecting the material losses [8]. Therefore, it is very important to validate the effective losses of the material before considering the antenna design. The considered SWCNTs

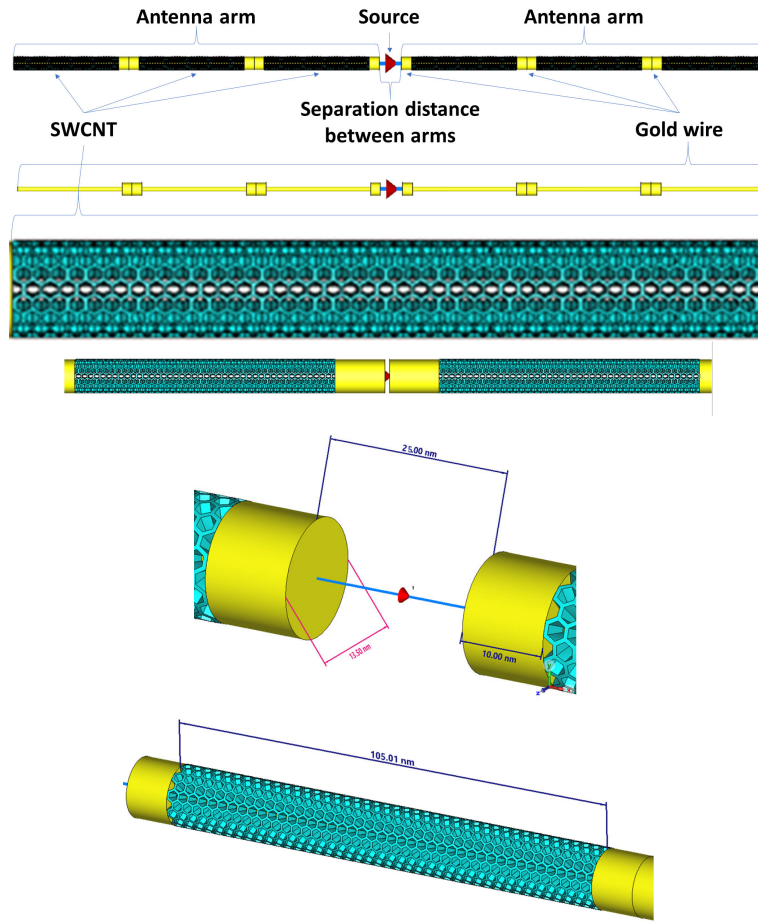


FIGURE 4. The proposed dipole antenna based plasmonic structure. Note that the dimensions are in nano-scale.

exhibit an effective permittivity, and their optical conductivity can be mathematically represented as follows [10]:

$$\epsilon_{eff}(\omega, \mu_c) = \epsilon_0 - \frac{i}{\omega} [\sigma_{intra}(\omega, \mu_c) + \sigma_{inter}(\omega, \mu_c)] \quad (1)$$

$$\sigma_{intra}(\omega, \mu_c) = \frac{2ie^2kBT}{\pi\hbar^2(\omega + i\tau^{-1})} \ln \left(2 \cosh \left(\frac{\mu_c}{2kBT} \right) \right) \quad (2)$$

where e is the elementary charge, kB the Boltzmann constant, and T the absolute temperature. Additionally, \hbar refers to the reduced Planck constant, ω the angular frequency of the incident electromagnetic wave, τ the relaxation time (electron scattering time), and μ_c the chemical potential at the Fermi level [10].

The interband conductivity of SWCNT represents the main part that is connected directly to the effects of the chemical potential difference. Also, it is considered the likelihood of the electrons charge density at the microscale phenomena that usually occurs at the plasmonic effects. Such a term can be explained by the following equation [5]:

$$\sigma_{intra}(\omega, \mu_c) = \frac{e^2}{\pi\hbar} \left[\frac{1}{2} + \frac{1}{\pi} \arctan \left(\frac{\hbar\omega - 2\mu_c}{2kBT} \right) - \frac{i}{2\pi} \ln \left(\frac{(\hbar\omega + 2\mu_c)^2}{(\hbar\omega - 2\mu_c)^2 + (2kBT)^2} \right) \right] \quad (3)$$

This will lead to more confidence with our model by involving the two curl Maxwell's equations that are given by [9]:

$$\nabla \times E(\omega) = i\omega\mu_0 H(\omega) \quad (4)$$

$$\nabla \times H(\omega) = -i\omega\epsilon_{eff}(\omega, \mu_c) \mu_0 \quad (5)$$

where ϵ_{eff} is the effective permittivity described in Equation (1). The total conductivity (σ) is:

$$\sigma(\omega, \mu_c) = \sigma_{intra}(\omega, \mu_c) + \sigma_{inter}(\omega, \mu_c) \quad (6)$$

with electric field ($E(\omega)$) and magnetic field ($H(\omega)$). These fields are now coupled through the modified Maxwell's equations, with ϵ_{eff} encapsulating the material's response due to quantum conductance [4]. The effective SWCNT relative permittivity is calculated according to the given Equation (1) and represented in Fig. 5.

$$\epsilon'_r = 1 + \frac{\sigma'_r}{\omega\epsilon_0} \quad (7)$$

$$\epsilon''_r = 1 + \frac{\sigma''_r}{\omega\epsilon_0} \quad (8)$$

We find from the evaluated permittivity within the frequency band of interest that the considered SWCNT shows a permittivity almost zero in real value around 500 THz with high losses

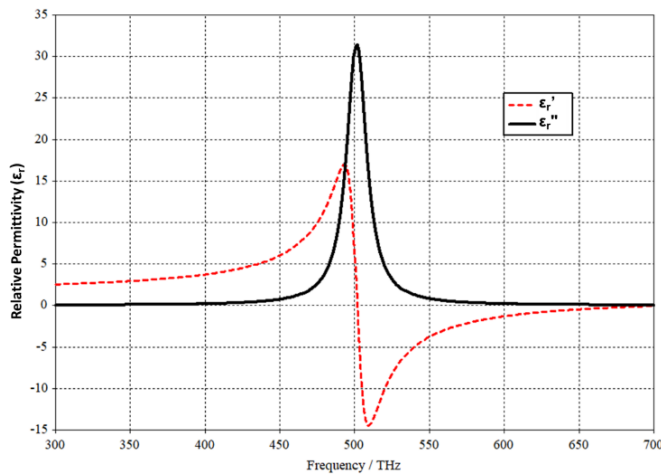


FIGURE 5. The evaluated effective relative permittivity within the frequency band of interest.

according to the imaginary part [6].

$$\begin{aligned} \sigma(\omega, \mu_c) &= \frac{2ie^2kBT}{\pi\hbar 2(\omega + i\tau^{-1})} \ln \left(2 \cosh \left(\frac{\mu_c}{2kBT} \right) \right) \\ &+ \frac{e^2}{\pi\hbar} \left[\frac{1}{2} + \frac{1}{\pi} \arctan \left(\frac{\hbar\omega - 2\mu_c}{2kBT} \right) \right. \\ &\left. - \frac{i}{2\pi} \ln \left(\frac{(\hbar\omega + 2\mu_c)^2}{(\hbar\omega - 2\mu_c)^2 + (2kBT)^2} \right) \right] \quad (9) \end{aligned}$$

$$\begin{aligned} \sigma(\omega, \mu_c\tau) &= \frac{2ie^2kBT}{\pi\hbar 2(\omega + i\tau^{-1})} \ln \left(2 \cosh \left(\frac{\mu_c}{2kBT} \right) \right) \\ &+ \frac{e^2}{\pi\hbar} \left[\frac{1}{2} + \frac{1}{\pi} \arctan \left(\frac{\hbar\omega - 2\mu_c}{2kBT} \right) \right. \\ &\left. - \frac{i}{2\pi} \ln \left(\frac{(\hbar\omega + 2\mu_c + i\hbar/\tau)^2}{(\hbar\omega - 2\mu_c + i\hbar/\tau)^2 + (2kBT)^2} \right) \right] \quad (10) \end{aligned}$$

The terms involving τ introduce a complex frequency shift, which broadens the resonance, and reduce the likelihood of sharp Interbrand transitions. The broadening of energy levels is modified by the scattering time τ which effects the interband transitions, particularly at higher frequencies [7]. Plasmonic resonance frequencies of single-walled carbon nanotubes (SWCNTs) vary depending on their structural and electronic properties, as well as environmental factors. Key determinants include the electronic type of SWCNT, nanotube diameter and chirality, environmental dielectric constant, and the length of the nanotube. Typical plasmonic frequencies range from 0.1 to 10 THz, making them ideal for THz photonics and sensing applications. Other factors for tuning frequency include doping, hybridization, and geometric modifications. For example, a metallic SWCNT with a diameter of ~ 1 nm typically has plasmonic resonances in the mid- to far-infrared range [20].

4. ANTENNA DESIGN METHODOLOGY

The optical antenna operation basically depends on two main criteria: The first is the frequency band of interest, which is relative to the antenna arm length ($\lambda/4$). This is the responsible condition of the electrical resonance. The second criterion is the effective gain, which is the amount of the radiated power from the antenna within a specific solid angle. Those two conditions are relative to the traditional electromagnetic theory. However, for the proposed study, the effects of the material behavior at the optical regime are an effective issue. First of all, the location of the plasmonic resonance from the electromagnetic spectrum is an important part of the design that sometimes must be avoided, which causes high losses. Next, the amount of real permittivity is an issue in the design that effects accordingly to the speed of light propagation, which in another expression changes the guided wavelength. All these considerations must be invoked during the antenna design that can be controlled by a parametric study during the simulation work.

The proposed antenna is designed for operation around frequency 600 THz, making it suitable for optical communication systems in the visible regime. For this, we conducted a parametric study to obtain such frequency band with an initial length of the proposed nano-dipole arm around 250 nm. This component is covered with a section based on SWCNT of (11,8 index). The two arms are separated with a gap to obtain a matching impedance bandwidth below 10 dB. As a result during the parametric study investigation, we varied the separation distance, the number of SWCNTs, and gold length according to those criteria (600 THz and -10 dB). The following sections describe the proposed study in details:

4.1. Section Number Effects

In this section, the number of SWCNT and gold sections is increased gradually to reach the desire frequency around 600 THz. We found with increasing the sections numbers a rapid decrease in the frequency resonance. This occurs because of electrical length increase that came from the traditional theory of antenna design [24]. Nonetheless, the suggested antenna shows a significant response to the SWCNT sections increase in terms of gain because of the influence of SWCNT plasmonic signature. This observation agrees well with the inherent characteristics of the SWCNT permittivity and permeability, which were described by quantum conductivity of the material. It should be noted during the design process to maintain the agreement between the electrical resonance and the plasmonic signature of the material that such agreement keeps the high performance of the antenna for our applications. Therefore, we increased the SWCNT and gold sections until we achieved the resonance around the plasmonic resonance frequency approximately 538 THz. The obtained results in terms of S_{11} and gain spectra are evaluated and presented in Fig. 6 and Fig. 7, respectively. It is obvious from the collected findings that the antenna shows a frequency resonance at 625 THz with a gain of 39 dBi. The acquired gain results are quite similar to those of standard dipole antenna; however, the effective size of the antenna is less than the traditional one with factor of $\lambda/4$.

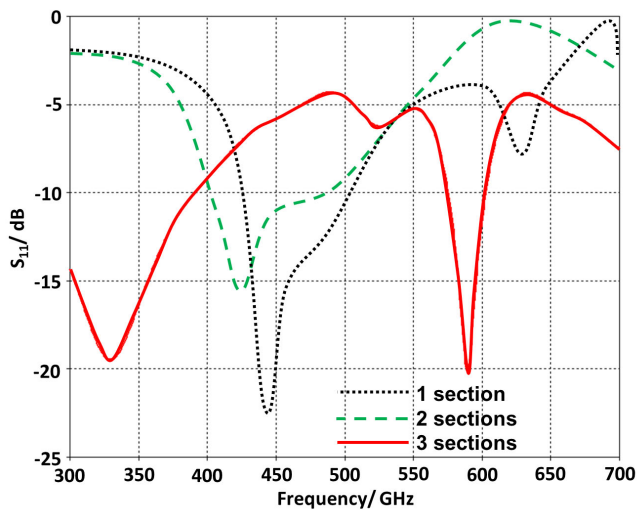


FIGURE 6. The evaluated S_{11} spectra of the proposed antenna with different SWCNT section numbers.

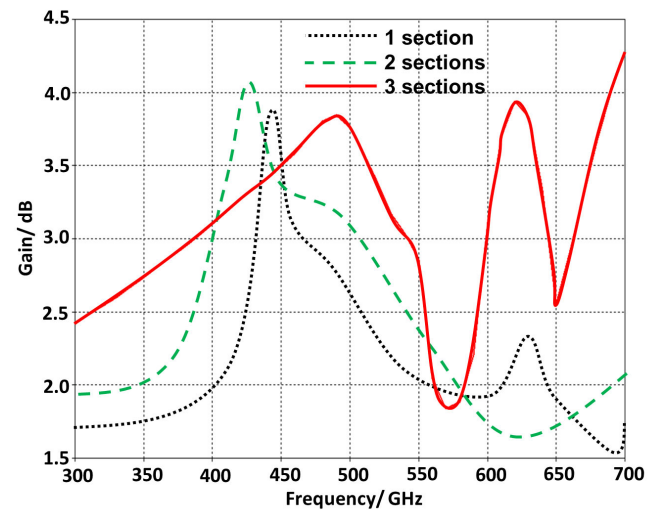


FIGURE 7. The evaluated gain spectra of the proposed antenna with different SWCNT section number.

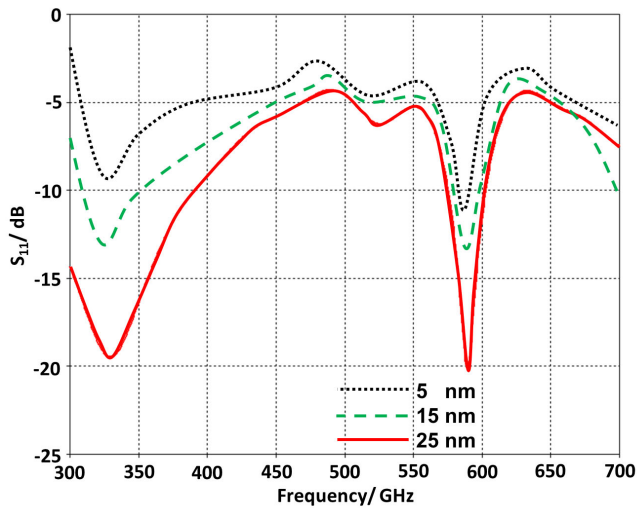


FIGURE 8. The evaluated S_{11} spectra of the proposed antenna with different separation distance.

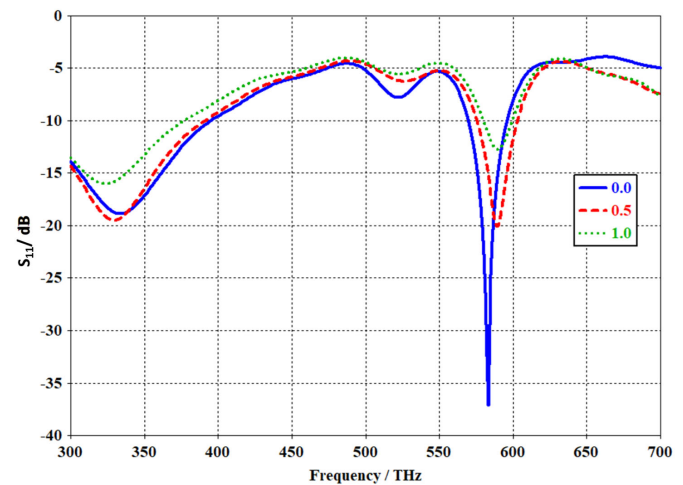


FIGURE 9. The evaluated S_{11} spectra of the proposed antenna with different chemical potential difference values.

Based on this, we analyzed the antenna gain, see Fig. 7, which describes the electromagnetic radiations around the antenna. We observed from the data gathered that the proposed radiation pattern corresponds to conventional one, which answers why the antenna has the same gain as the old one. Indeed, the electromagnetic radiation pattern is the responsible property for the antenna gain enhancement. It is important to emphasize that each SWCNT arm length is kept to $\lambda/4$ that is equivalent to 250 nm.

4.2. Separation Gap Effects

It is well known that the separation distance between the antenna arms is the responsible part of the matching performance. The authors disused this matter by changing such distance from 5 nm to 30 nm, and we found that no noticeable change occurred in the matching impedance. This is due to the coupling of ca-

pacitors between antenna arms, which reflects the effects on the antenna matching impedance with a change on the imaginary part, hence maintaining the antenna bandwidth relative to S_{11} below 10 dB. Furthermore, it is found that such variation in the antenna matching impedance could be attributed to the electrostatic charge accumulations within the gap distance between arms. The evaluated S_{11} spectra with respect to varying the separations distance is depicted in Fig. 8, for all parametric attempts.

5. EFFECTS OF CHANGING THE CHEMICAL POTENTIAL

The authors applied parametric study to demonstrate the consequences of modifying the chemical potential on the antenna performance in terms of S_{11} spectra, gain spectra, and radiation patterns, as shown in Fig. 9. In this paper, we applied a

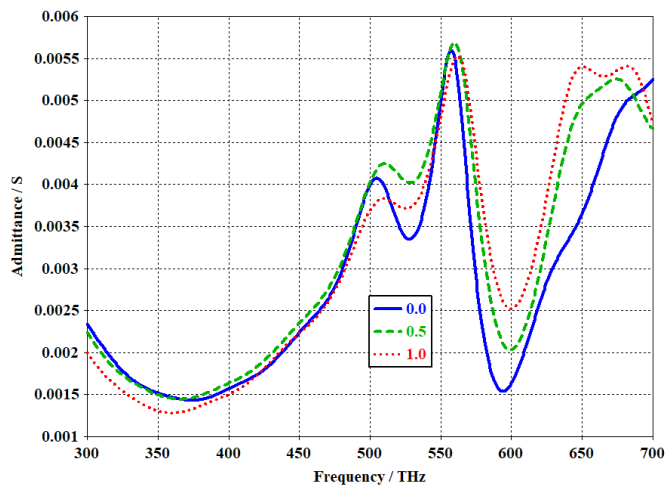


FIGURE 10. The evaluated admittance spectra of the proposed antenna with different chemical potential difference values.

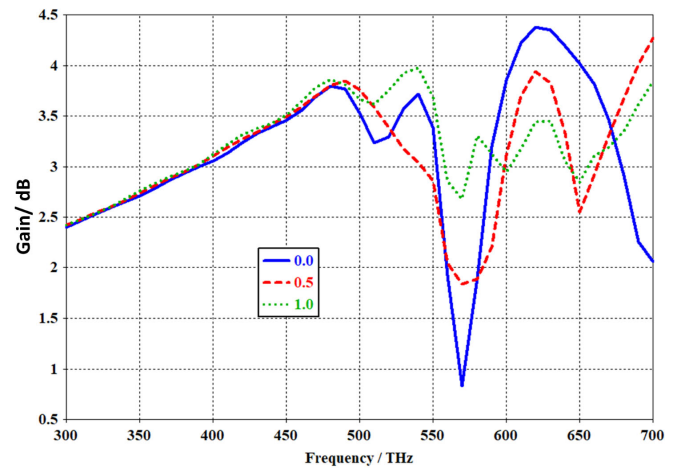


FIGURE 11. The evaluated gain spectra of the proposed antenna with different chemical potential difference values.

TABLE 1. The evaluated permittivity and phase change according to the considered chemical potential change.

Chemical potential voltage (e.V)	ϵ_r (real)	ϵ_r (imaginary)	$\beta(\pi)$	β (degree)
0.0	0.31	1.01	0.067	12.06
0.1	3.01	1.51	0.8	144
0.2	5.99	3.11	0.527	102.96
0.3	9.00	4.52	0	0
0.4	11.98	6.01	0.44	79.2
0.5	14.98	7.63	0.58	104.4
0.6	17.98	9.15	0.97	174.6
0.7	20.98	10.53	0.73	131.4
0.8	23.98	12.29	0.26	46.8
0.9	26.97	13.72	0.28	50.4
1.0	29.97	15.25	0.36	64.8

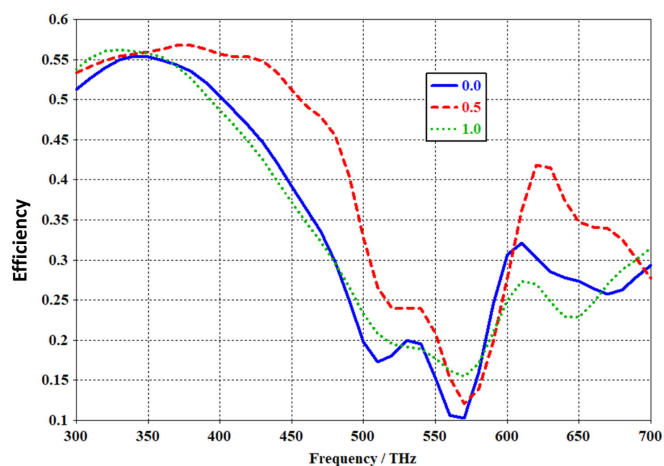


FIGURE 12. The evaluated antenna efficiency spectra of the proposed antenna with different chemical potential difference values.

study to compute the effect of varying the chemical potential effect on the real permittivity, imaginary permittivity, and phase change in terms of degree and radian. It is good to mention that

such biasing process to control the SWCNT performance can be achieved by applying two electrodes as the same technique suggested in [24]. These calculations are listed in Table 1. From the computed findings we found a significant effect on varying the material permittivity with changing the chemical potential level. Such observations are found to be very effective in calculating the phase change that could be very useful during the antenna beam steering and will be discussed later. It is good to mention that the proposed antenna is mainly of SWCNT that is highly affected by the chemical potential difference in which any variation in one of SWCNT segments realizes detectable change in the antenna effective phase to be investigated during beam steering. The main reason of such change occurring in the phase difference is attributed to variation in Fermi velocity that restricts the plasmonic charge motion on such material. Consequently, this may lead to reduction in the electromagnetic speed due to the electron population in valance band increase in the crystal lattice.

The evaluated admittance is found to vary with respect to the change in the chemical potential difference as seen in Fig. 10. The main advantage is that such change realizes insignificant

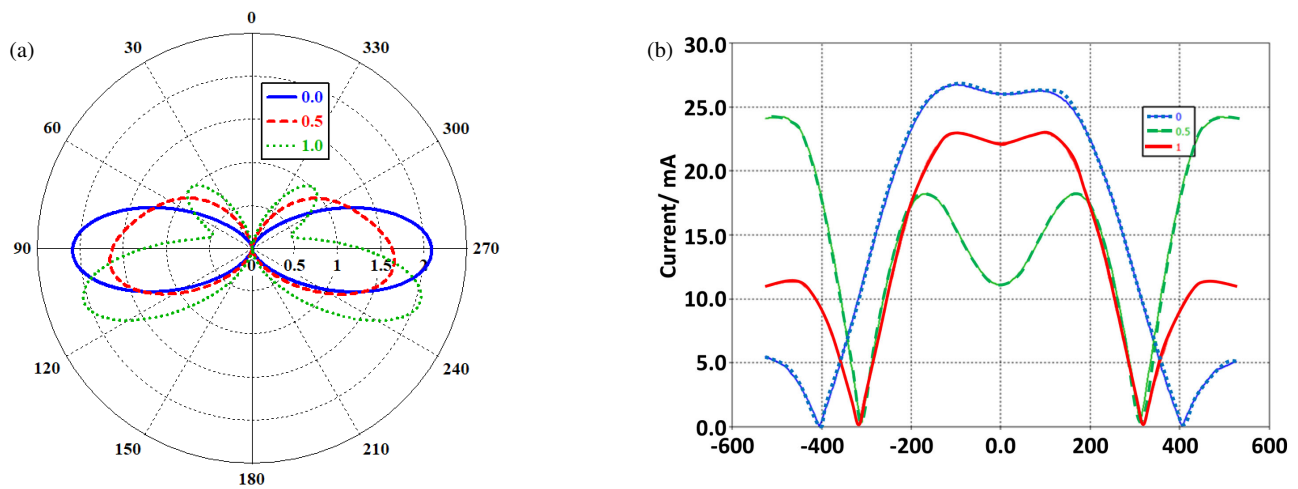


FIGURE 13. (a) Antenna radiation patterns change with changing chemical potential differences. (b) Antenna surface current change with changing chemical potential differences.

TABLE 2. A comparison table between the proposed work and other published results.

Ref.	Antenna type	Antenna size	Material	Frequency Band	Application
[19]	broadband optical nano-antenna	1600 × 1600 nm ²	AG, Si, SiO ₂	(666 to 6000 nm)	optical energy harvesting applications
[20]	flower shaped nano dipole antenna	1000 × 1000 nm ²		170 to 271 THz	optical wireless communication
[18]	Optical Nano-Antenna	Si (850, 625, and 300) nm, AG (1100, 1100, 200) nm, SiO ₂ (1100, 1100, and 8680)	AG, Si, SiO ₂	193.5 THz	photo-detection, nonlinear plasmonic, medicine, and energy-harvesting applications
[17]	Nano hybrid plasmonic antenna	1100 × 800 nm ²	Silicon-on-(Insulator)	160–240 THz	utilized for photo emission, optical detection, optically sensing, energy harvesting
[23]	nano-antenna based on Acer leaf with Y-shaped transmission line	49 × 49 nm ² with thickness of 1 nm	Si, Au and graphene	500 THz	Optical reconfigurable application
Our work	Dipole antenna	250 nm	Copper and SWCNT	600 THz	Optical reconfigurable application

variation in the matching to confirm that the proposed antenna resonance would be not affected with material properties change.

The antenna gain spectra are evaluated with varying the chemical potential difference value as depicted in Fig. 11. We found that the proposed antenna realizes a tunable gain from 3 dBi to 4 dBi at 535 THz and almost from 3.5 dBi to 4.3 dBi at 625 THz with respect to changing the chemical potential. Such change is due to the effects of the material loss change.

Next, the effects of changing the chemical potential differences on the antenna efficiency are evaluated as seen in Fig. 12. It is found that the proposed antenna efficiency shows almost no significant variation with respect to the considered frequencies. This is because antenna radiation efficiency is usually independent of the material properties, but indeed, it mainly depends on the electromagnetic coupling aperture.

In Fig. 13(a), the antenna radiation patterns are evaluated with respect to the change in the chemical potential differences. It is found that a significant change occurs with varying the chemical potential differences [25]. Such change is attributed to the effects of effective change in the surface current distribution as seen in Fig. 13(b). This variation in the antenna gain could nominate the proposed antenna to be excellent candidate to modern application including direct optical modulation process as in microwave bands [26].

From our calculations of the proposed antenna performance compared to other published results in the literature, we discovered that the suggested design realized significant enhancements in the antenna size, as listed in Table 2. In this table, we listed the comparison in the antenna type, material, and frequency with respect to applications. We found that the proposed

antenna showed significant advancements in comparison to the listed antenna types.

6. CONCLUSION

In this work, the design of a reconfigurable dipole plasmonic antenna is considered for an optical communication system at visible regime. The proposed antenna is designed for the first time in the literature by considering the realistic shape with SWCNT and filled with nano copper arms to realize beam forming from changing the surface current on the dipole surface. The antenna is built with two arms, and each arm is constructed from segments of SWCNT and three segments of gold. Such a configuration realized a significant enhancement in the antenna performance and size reduction. We discussed the impacts of the changing the chemical potential on the antenna performance; from that, we explored that there is a high impact of changing the chemical potential on the antenna beam steering due to the chemical potential change. We established the relationship with respect to each antenna parameter. It is found that the proposed antenna realized a significant enhancement in terms of size reduction. The antenna offers a frequency resonance at 600 THz with a dipole length of 750 nm with gain almost 4 dBi. The proposed antenna shows enhanced bandwidth with frequency tuning around 200 THz with excellent response to the chemical potential change. Nevertheless, the antenna is found to show excellent beam forming response to the variation in the chemical potential difference. This response is attributed to variation in the surface current change. Such ability could be a promising technology for several future applications including optical communication systems and direct antenna modulation based on ON/OFF Keying (OOK) schema by manipulating the light intensity. Finally, from utilizing resonant plasmonic effects at 600 THz, the antenna achieves a radiation efficiency about 57% beam steering up to $\pm 25^\circ$ from the central axis with narrow beamwidth around 10° and low front to back ratio and side lobes at the resonance.

REFERENCES

- [1] Jassim, D. A. and T. A. Elwi, "Optical nano monopoles for interconnection electronic chips applications," *Optik*, Vol. 249, 168142, 2022.
- [2] Hanson, G. W., "Dyadic Green's functions and guided surface waves for a surface conductivity model of graphene," *Journal of Applied Physics*, Vol. 103, No. 6, 064302, 2008.
- [3] Tizani, L., Y. Abbas, A. M. Yassin, B. Mohammad, and M. Rezeq, "Single wall carbon nanotube based optical rectenna," *RSC Advances*, Vol. 11, No. 39, 24 116–24 124, 2021.
- [4] Hasan, R. R., A. M. Saleque, A. B. Anwar, M. A. Rahman, and Y. H. Tsang, "Multiwalled carbon nanotube-based on-body patch antenna for detecting COVID-19-affected lungs," *ACS Omega*, Vol. 7, No. 32, 28 265–28 274, 2022.
- [5] Sharma, A. K., A. K. Sharma, and R. Sharma, "Model study of complex conductivity and permittivity of CNT/PANI composite (CPC) material for application of THz antenna," *Materials Today: Proceedings*, Vol. 46, 5833–5837, 2021.
- [6] Ren, X., Z. Ji, B. Chen, J. Zhou, Z. Chu, and X. Chen, "Carbon nanotube far infrared detectors with high responsivity and superior polarization selectivity based on engineered optical antennas," *Sensors*, Vol. 21, No. 15, 5221, 2021.
- [7] Ren, X., J. Zhou, X. Chen, H. Li, and R. Dong, "Metamaterial optical antennas powered carbon nanotube detectors with extremely high polarization selectivity," in *Third International Conference on Optoelectronic Science and Materials (ICOSM 2021)*, Vol. 12030, 143–147, Hefei, China, 2021.
- [8] Yoo, S., S. Zhao, and F. Wang, "Infrared light-emitting devices from antenna-coupled luttinger liquid plasmons in carbon nanotubes," *Physical Review Letters*, Vol. 127, No. 25, 257702, 2021.
- [9] Suzuki, D., Y. Takida, Y. Kawano, H. Minamide, and N. Terasaki, "Carbon nanotube-based, serially connected terahertz sensor with enhanced thermal and optical efficiencies," *Science and Technology of Advanced Materials*, Vol. 23, No. 1, 424–433, 2022.
- [10] Elwi, T. A. and H. M. Al-Rizzo, "Electromagnetic wave interactions with 2D arrays of single-wall carbon nanotubes," *Journal of Nanomaterials*, Vol. 2011, No. 1, 709263, 2011.
- [11] Jurn, Y. N., "Bandwidth optimization of single-walled carbon nanotube dipole antenna at GHz frequency regime," *International Journal of Advanced Engineering, Management and Science*, Vol. 8, 9, 2022.
- [12] Biris, A. S., H. Al-Rizzo, T. Elwi, and D. Rucker, "Nano and micro based antennas and sensors and methods of making same," US Patent 8,692,716, 2014.
- [13] Madany, Y. M., "Investigation and analysis of nanowire antennas for terahertz frequency range applications," in *2022 International Telecommunications Conference (ITC-Egypt)*, 1–10, Alexandria, Egypt, 2022.
- [14] Moshiri, S. M. M. and N. Nozhat, "Smart optical cross dipole nanoantenna with multibeam pattern," *Scientific Reports*, Vol. 11, No. 1, 5047, 2021.
- [15] Saleem, A. E. and J. A. Hasan, "Metamaterial-based nanoantenna design of enhanced plasmonic electromagnetic properties," *Tikrit Journal of Engineering Sciences*, Vol. 31, No. 3, 266–274, 2024.
- [16] Aziz, F. H. and J. A. Hasan, "Design and simulation of a graphene material-based tuneable nanoantenna for THz applications," in *International Conference on Innovative Computing and Communications (ICICC 2024)*, 1–13, New Delhi, India, Feb. 2024.
- [17] Tejasree, M., A. Taguru, M. Praneetha, K. Naveen, P. V. Naidu, et al., "Hybrid plasmonic nano-antenna design and analysis for optical applications," in *2022 IEEE Delhi Section Conference (DELCON)*, 1–4, New Delhi, India, Feb. 2022.
- [18] Elwi, T. A., "Novel antennas based on innovations in nano-scale and metamaterial structures," Ph.D. dissertation, University of Arkansas (UALR), Arkansas, USA, 2011.
- [19] Elwi, T. A., N. M. Noori, and M. N. Majeed, "On the performance of adaptive intelligent wireless sensor nodes nanostructured array for IoT applications," *International Journal of Telecommunications & Emerging Technologies*, Vol. 9, No. 2, 29–39, 2023.
- [20] Merlo, J. M., N. T. Nesbitt, Y. M. Calm, A. H. Rose, L. D'Imperio, C. Yang, J. R. Naughton, M. J. Burns, K. Kempa, and M. J. Naughton, "Wireless communication system via nanoscale plasmonic antennas," *Scientific Reports*, Vol. 6, No. 1, 31710, 2016.
- [21] Olmos-Trigo, J., H. Sugimoto, and M. Fujii, "Far-field detection of near-field circular dichroism enhancements induced by a nanoantenna," *Laser & Photonics Reviews*, Vol. 18, 2300948, 2024.

- [22] Yaroshenko, V., M. Obramenko, A. Dyatlovich, P. Kustov, A. Gudovskikh, A. Goltaev, I. Mukhin, E. Ageev, and D. Zuev, “Active erbium-doped silicon nanoantenna,” *Laser & Photonics Reviews*, Vol. 17, No. 4, 2200661, 2023.
- [23] Jalil, S. A., K. M. Awan, J. Baxter, G. Bart, D. N. Purschke, T. Fennel, D. M. Villeneuve, A. Staudte, P. Berini, T. Brabec, L. Ramunno, and G. Vampa, “Spectroscopic signatures of plasmonic near-fields on high-harmonic emission,” *Laser & Photonics Reviews*, Vol. 17, No. 12, 2300448, 2023.
- [24] Calò, G., G. Bellanca, A. E. Kaplan, P. Bassi, and V. Petruzzelli, “Double Vivaldi antenna for wireless optical networks on chip,” *Optical and Quantum Electronics*, Vol. 50, 261, 2018.
- [25] Saleem, A. E. and J. A. Hasan, “Steerable nano-antenna array based plasmonic quantum capacitor for optical band application,” in *2024 International Conference on Distributed Computing and Optimization Techniques (ICDCOT)*, 1–6, Bengaluru, India, Mar. 2024.
- [26] Jwair, M. H. and T. A. Elwi, “Steerable composite right-left-hand-based printed antenna circuitry for 5G applications,” *Microwave and Optical Technology Letters*, Vol. 65, No. 7, 2084–2091, 2023.